J. Fluid Mech. (1972), *vol.* 56, *part* 1, *pp.* 121–141
Printed in Great Britain

Three-dimensional MHD duct flows with strong transverse magnetic fields. Part 3. Variable-area rectangular ducts with insulating walls

By J. S. WALKER
Department of Theoretical and Applied Mechanics, University of Illinois
G. S. S. LUDFORD
Department of Theoretical and Applied Mechanics, Cornell University
AND J. C. R. HUNT
Department of Applied Mathematics and Theoretical Physics, Cambridge University

(Received 29 May 1972)

The general analysis developed in Parts 1 and 2 of three-dimensional duct flows subject to a strong transverse magnetic field is used to examine the flow in diverging ducts of rectangular cross-section, the walls of which are electrically non-conducting. A dramatically different flow is found in this case from that studied in Part 2, where the side walls parallel to the magnetic field were highly conducting. Now it is found that the core velocity normalized with respect to the mean velocity is of $O(M^{-\frac{1}{2}})$ while the velocity in the side-wall boundary layers is of $O(M^{\frac{1}{2}})$, so that these boundary layers carry most of the flow. The problem of entry is solved by analysing the change from fully developed Hartmann flow in a rectangular duct to the flow in the diverging duct. It is found that the disturbance in the upstream duct decays exponentially. The analysis of the side-wall boundary layers is more difficult than that in Part 1 on account of the different boundary conditions and requires the solution of two coupled integro-differential equations. Numerical solutions are obtained for a duct whose width increases linearly in the flow direction.

1. Introduction

In Part 1, Hunt & Ludford (1968) developed the general analysis of three-dimensional duct flows subject to a transverse magnetic field sufficiently strong for inertial effects to be negligible, and applied this analysis to flows past obstacles in channels of constant area. In Part 2, Walker, Ludford & Hunt (1971) considered variable-area symmetric rectangular ducts whose side walls (parallel to the applied magnetic field) are perfect conductors, the other (top and bottom) walls being insulators. They found that the essential problem was to determine the

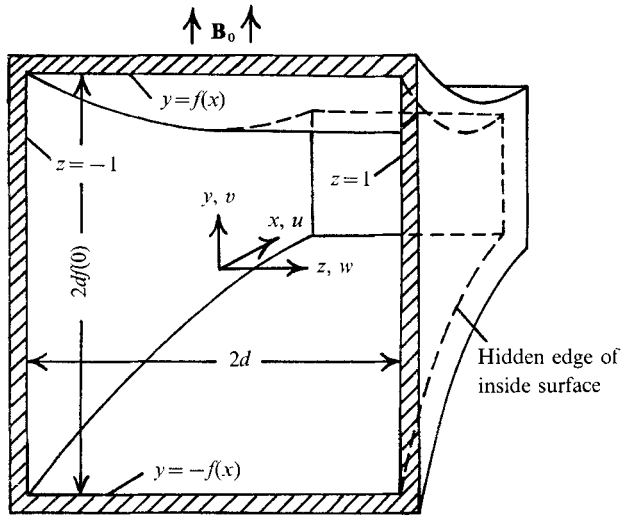

FIGURE 1. Duct with insulating walls.

structure of thin viscous boundary layers adjacent to the side walls and that the completely local character of these side layers made the analysis tractable for all three general types of such ducts. The analysis for similar ducts with insulating side walls turns out to be much more difficult because the local character of the flow is lost. However, the problem cannot be ignored since it is of fundamental importance in pumping liquid metals across strong magnetic fields, as in the cooling system of a fusion-power reactor (cf. Hunt & Hancox 1971) or the circulating system of an MHD generator. We first concentrate on ducts with parallel side walls and straight, diverging top and bottom walls, and then extend the analysis for this prototype to general fully insulated, variable-area rectangular ducts.

In §2 we derive the fundamental boundary-value problem governing the side layers in ducts with parallel side walls and diverging (or converging) top and bottom walls. When the side walls are insulating quite a different flow pattern can be expected, because the transverse currents generated in the core are now blocked. In constant-area rectangular ducts (see Hunt & Shercliff 1971) these currents simply recirculate in the y,z plane (figure 1) through the Hartmann layers at top and bottom. However, in a diverging duct the varying core velocity leads to a change in the induced electric field along the duct, and this basic difference causes the currents to circulate in the x,z plane through the core and side-wall layers. Since the latter are thicker and hence of lower resistance than the Hartmann layers, larger currents circulate (as in a constant-area duct, whose highly conducting top and bottom walls short circuit the Hartmann layers). This leads to high velocities in the side layers, which thereby carry nearly the entire flow.

Such jet-like velocity profiles have been found in two experiments undertaken at Riga. In the first (Branover & Shcherbinin 1966) the duct had a step increase in y (parallel to the magnetic field) at $x = 0$. It was found that most of the

flow hugged the side walls for $x > 0$, as if avoiding the expansion in the centre. In the second experiment (Slyusarev, Shilova & Shcherbinin 1970) the duct diverged in the y direction at 5°. (Note that although the top and bottom walls were made of stainless steel they had an insulating coating.) While such small divergences require a slightly modified theory, the predicted high velocity side layers were observed.

The opportunity is taken in §2 to revise the conditions at a Hartmann layer on a general insulating boundary, since the ones given in Part 1 erroneously neglected the surface curvature. This error does not affect any of the results presented in the MHD literature including the present paper, since all MHD analysis has been restricted to first-order approximations which are independent of surface curvature.

In §3 we reduce the side-layer problem to a pair of coupled integro-differential equations in x and y, where the applied magnetic field is in the y direction and the centre line of the duct is taken as the x axis (see figure 1). The presence of x derivatives in these equations reflects the loss of the local character of the flows treated in Part 2. A single integro-differential equation is derived for the solution in the diverging portion of a prototype with top and bottom walls at $y = \pm a$ for $x < 0$ and at $y = \pm (a + bx)$ for $x > 0$. The physical situation is quite different in the constant-area portion ($x < 0$) since the fluid outside the side layers can have any irrotational motion in the x, z plane when the top and bottom walls are parallel (see Part 1). The upstream ($x < 0$) influence of the divergence is restricted to the neighbourhood of the join at $x = 0$ and the fully developed solution is recovered sufficiently far away from the join. In the fully developed solution for an insulated rectangular duct there are no high velocity side layers and the non-dimensional core velocity is equal to one everywhere. As we approach the join, part of the mass flux is drawn into the side-layer regions, so that high velocity layers develop before the divergence begins and locally disturb the fully developed flow. The integro-differential equation derived in §3 is singular in the limit $b \to 0$ and a new equation is derived in §4 for the high velocity side layers in the constant-area portion.

In §5 we derive an integral relationship between the upstream and downstream side-layer solutions evaluated at $x = 0$. The numerical solution presented in §6 involves expanding the two solutions in the eigenfunctions of the two integro-differential equations and using the joining integral equation to determine the coefficients in these expansions. With the proper scaling in $a + bx$, the variables in the diverging portion are independent of x except in the neighbourhood of the join. In §7 we present typical profiles for the high velocity side layers in this quasi-developed solution, which was originally derived in Walker's thesis (1970). The flow near the join is quite complex, but the severity of the disturbance here is reflected in a plot of the fraction of the total mass flux carried by the high velocity side layers in the constant-area portion as a function of the divergence b.

In §8 we discuss the extension of the analysis for this prototype to other fully insulated rectangular ducts.

2. Formulation of the problem for a general duct

If the induced magnetic field and the fluid inertia are negligible, the non-dimensional equations governing the steady flow of an electrically conducting liquid of uniform properties under the action of a transverse magnetic field $\mathbf{B}_0 = B_0\hat{\mathbf{y}}$ are

$$\nabla h = \mathbf{j}\times\hat{\mathbf{y}} + M^{-2}\nabla^2\mathbf{v}, \quad \nabla.\mathbf{v} = 0,$$
$$\mathbf{j} = \nabla\phi + \mathbf{v}\times\hat{\mathbf{y}}, \quad \nabla.\mathbf{j} = 0$$

(see Part 2). Here h is the rescaled pressure p/N, $\mathbf{j}$ is the electric current density, $\mathbf{v}$ is the fluid velocity, ϕ is the electric potential and $N = \sigma B_0^2 d/\rho U_0$ and $M = B_0 d(\sigma/\eta)^{\frac{1}{2}}$ are the interaction and Hartmann numbers respectively. The induced magnetic field can be neglected when the magnetic Reynolds number $R_m = \mu U_0 \sigma d$ is small and, for the present problem, the inertial effects can be neglected when $N \gg M^{\frac{3}{2}}$ or $N \gg R^3$ or $M^{\frac{1}{2}} \gg R$,

where $R = M^2/N = \rho U_0 d/\eta$ is the Reynolds number (see Part 2, p. 682 for limitations of this approximation). The governing equations are equivalent to

$$\partial^2\phi/\partial y^2 = M^{-2}\nabla^4\phi, \quad \partial v/\partial y = \nabla^2 h, \quad \partial h/\partial y = M^{-2}\nabla^2 v, \qquad (1a,b,c)$$
$$u = -\partial\phi/\partial z - \partial h/\partial x + M^{-2}\nabla^2 u, \quad w = \partial\phi/\partial x - \partial h/\partial z + M^{-2}\nabla^2 w, \qquad (1d,e)$$
$$j_x = \partial h/\partial z - M^{-2}\nabla^2 w, \quad j_y = \partial\phi/\partial y, \quad j_z = -\partial h/\partial x + M^{-2}\nabla^2 u, \qquad (1f,g,h)$$

where the first two equations are obtained by substituting the other equations into $\nabla.\mathbf{v} = \nabla.\mathbf{j} = 0$.

The present duct (shown in figure 1) has parallel plane side walls, so that half their distance apart will be taken for the characteristic length d. The average velocity at some section, say $x = 0$, will be used for the characteristic velocity U_0. Thus

$$\int_{-1}^{+1}\int_{-f(0)}^{+f(0)} u(0,y,z)\,dy\,dz = 4f(0). \qquad (2)$$

As boundary conditions we have

$$\mathbf{v} = 0, \quad j_y = \pm f'(x) j_x \quad \text{at} \quad y = \pm f(x), \qquad (3a)$$

and

$$\mathbf{v} = 0, \quad j_z = 0 \quad \text{at} \quad z = \pm 1. \qquad (3b)$$

Together with the governing equations (1) these form a homogeneous problem whose solution is normalized by the condition (2). The Hartmann number is the only parameter in this problem and under the assumption that $M \gg 1$ the flow region may be divided into a central core and thin boundary layers in the fluid adjacent to the duct walls. The various subregions (shown in figure 2) are (*a*) the core, (*b*) primary Hartmann layers, (*c*) side layers, (*d*) secondary Hartmann layers and (*e*) corner regions.

The core variables, denoted by capital letters, satisfy equations (1) neglecting $O(M^{-2})$ terms, so that

$$\left.\begin{aligned} &\Phi = y\Omega + \Psi, \quad U = -y(\partial\Omega/\partial z) - \partial H/\partial x - \partial\Psi/\partial z, \\ &V = y(\partial^2 H/\partial x^2 + \partial^2 H/\partial z^2) + G, \quad W = y(\partial\Omega/\partial x) + \partial\Psi/\partial x - \partial H/\partial z, \\ &J_x = \partial H/\partial z, \quad J_y = \Omega, \quad J_z = -\partial H/\partial x, \end{aligned}\right\} \qquad (4)$$

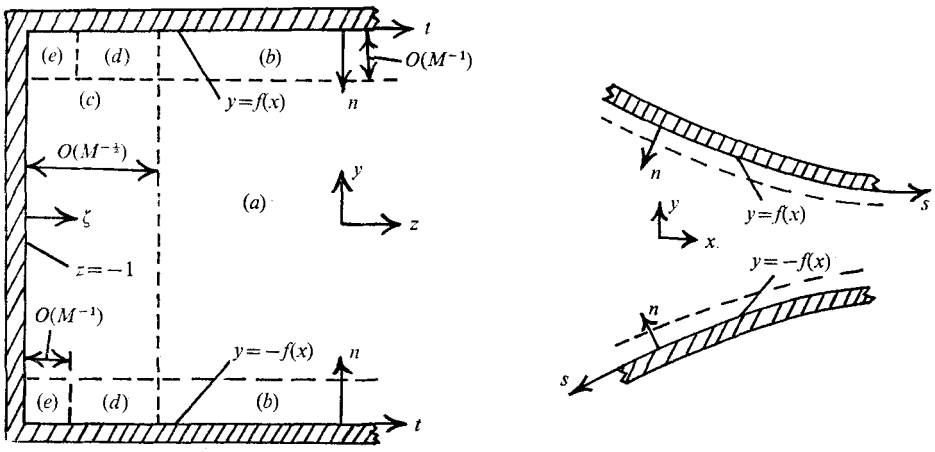

FIGURE 2. x and z sections showing subregions and notation.

where Ω, Ψ, H, and G are integration functions of x and z (H being the core pressure). The variables in the primary Hartmann layers are determined locally from the tangential velocity and current outside, and match the core variables provided that the latter satisfy certain boundary conditions, which physically express the conservation of mass and charge within the layer.

For a general insulator which is nowhere tangential to the applied magnetic field, we write the governing equations in an orthogonal curvilinear co-ordinate system (n, s, t), where s and t follow the surface's lines of curvature and n is the distance along the normal. Since the layer thickness is of $O(M^{-1})$ we stretch the n co-ordinate by M and expand the variables as power series in M^{-1}. The solution has a local exponential structure

$$\exp(-|\cos\alpha|Mn) \quad \text{where} \quad \alpha(s,t) = \arccos(\hat{\mathbf{n}}.\hat{\mathbf{y}}),$$

and satisfies the boundary conditions (3a), namely

$$\mathbf{v} = 0, \quad j_n = 0 \quad \text{at} \quad Mn = 0,$$

provided that the core solution (which it matches as $Mn \to \infty$) satisfies the boundary conditions

$$\left.\begin{aligned} V_n &= (h_s h_t M)^{-1}(\partial(h_t V_s|\sec\alpha|)/\partial s + \partial(h_s V_t|\sec\alpha|)/\partial t) \\ J_n &= (h_s h_t M)^{-1}\operatorname{sgn}(\cos\alpha)(\partial(h_t V_t)/\partial s - \partial(h_s V_s)/\partial t) \end{aligned}\right\} \quad \text{at} \quad n = 0. \qquad (5)$$

Here $h_s^2 ds^2 + h_t^2 dt^2$ is the square of the line element on the surface. The Hartmann conditions (5) differ from the corresponding equations (2.24) and (2.27) of Part 1, equations (8) of Part 2, and equation (2.13) of Kulikovskii (1968) which were wrong for any situation where α (and hence the layer thickness $M^{-1}|\sec\alpha|$) or h_s or h_t varies along a surface. This error does not affect the analysis in either of those parts or Kulikovskii's paper since V_n was only calculated to $O(1)$ and $h_s = h_t = 1$ for the duct walls considered.

In our case the s axis is curved (see figure 2) but since we shall again neglect $O(M^{-1})$ terms the Hartmann boundary conditions (5) are simply

$$f'U \mp V = 0, \quad f'J_x \mp J_y = 0 \quad \text{at} \quad y = \pm f(x).$$

The core variables (4) which satisfy them are (as in Part 2)

$$\left.\begin{aligned} &\Phi = \Psi - z(f')^{-1}\frac{d}{dx}\left(f\frac{dH}{dx}\right), \quad U = f(f')^{-1}\frac{d^2H}{dx^2}, \\ &V = y\frac{d^2H}{dx^2}, \quad W = \frac{\partial\Phi}{\partial x}, \quad J_x = J_y = 0, \quad J_z = -\frac{dH}{dx}, \end{aligned}\right\} \tag{6}$$

where Ψ and H are now functions of x alone.

If $J_z = O(1)$ then the continuity of current implies that j_x and j_y are of $O(M^{\frac{1}{2}})$ inside the side layers since the thickness of these layers is $O(M^{-\frac{1}{2}})$. Thus $(1g)$ implies that ϕ is of $O(M^{\frac{1}{2}})$ and $(1d)$ implies that u is of $O(M)$. This implies that the side layers carry an $O(M^{\frac{1}{2}})$ mass flux which contradicts the condition (2). Therefore in the side layers j_x, j_y and ϕ are of $O(1)$, u is of $O(M^{\frac{1}{2}})$ and the mass flux is of $O(1)$, while in the core J_z is of $O(M^{-\frac{1}{2}})$. The $O(1)$ part of H vanishes and the only non-zero $O(1)$ core variables are $\Phi = \Psi(x)$ and $W = d\Psi/dx$. Since the $O(1)$ part of U is zero, there is no $O(1)$ mass flux in the core and the entire $O(1)$ mass flux is carried by the side layers. Ψ represents a transfer of mass flux between the side layers and can be shown to be of $O(M^{-1})$ by applying the minimum dissipation theorem to an arbitrary length of duct (see Walker's thesis). Thus all $O(1)$ core variables vanish and the $O(M^{-\frac{1}{2}})$ core variables are given by expressions (6) with $\Psi = 0$ and $H(x)$ determined by matching the side-layer solutions at $z = \pm 1$.

The flow is symmetric in z so each side layer carries half the total mass flux $4f(0)$ and we need only consider the layer at $z = -1$. The substitution $\zeta = M^{\frac{1}{2}}(z+1)$ stretches the co-ordinate normal to the side wall giving a semi-infinite region with the insulator at $\zeta = 0$. The equations $(1a, b, c)$ governing ϕ, the $O(1)$ electric potential, v, the $O(M^{\frac{1}{2}})$ y velocity and h, the $O(M^{-\frac{1}{2}})$ rescaled pressure, are

$$\partial^2\phi/\partial y^2 = \partial^4\phi/\partial\zeta^4, \quad \partial v/\partial y = \partial^2 h/\partial\zeta^2, \quad \partial h/\partial y = \partial^2 v/\partial\zeta^2, \tag{7a,b,c}$$

while u, the $O(M^{\frac{1}{2}})$ x velocity, w, the $O(1)$ z velocity, j_x, the $O(1)$ x current, j_y, the $O(1)$ y current, and j_z, the $O(M^{-\frac{1}{2}})$ z current, are given by equations $(1d, e, f, g, h)$, namely

$$u = -\partial\phi/\partial\zeta, \quad w = \partial\phi/\partial x - \partial h/\partial\zeta, \quad j_x = \partial h/\partial\zeta, \tag{7d,e,f}$$

$$j_y = \partial\phi/\partial y, \quad j_z = -\partial h/\partial x - \partial^3\phi/\partial\zeta^3. \tag{7g,h}$$

The boundary conditions $(3b)$ for an insulator become

$$\partial\phi/\partial\zeta = v = \partial\phi/\partial x - \partial h/\partial\zeta = \partial h/\partial x + \partial^3\phi/\partial\zeta^3 = 0 \quad \text{at} \quad \zeta = 0. \tag{8a,b,c,d}$$

The Hartmann conditions (5) also apply in the side layers, where they yield

$$f'u \mp v = 0, \quad f'j_x \mp j_y = \partial u/\partial\zeta + f'\partial v/\partial\zeta \quad \text{at} \quad y = \pm f(x)$$

or

$$f'\partial\phi/\partial\zeta + v = \partial^2\phi/\partial\zeta^2 \mp \partial\phi/\partial y + f'\partial h/\partial\zeta \mp f'\partial v/\partial\zeta = 0 \quad \text{at} \quad y = \pm f(x), \tag{9}$$

and matching the core gives

$$v = \phi = 0, \quad h = H(x) \quad \text{as} \quad \zeta \to \infty. \tag{10}$$

Note that, to conserve notation, the dependent variables now denote the leading coefficient functions in their own expansions.

3. Integro-differential equation for a duct with straight walls

The equations (7*b*) and (10) can be satisfied by introducing a second potential function $\theta(x, y, \zeta)$ defined by

$$v = -f'\partial\theta/\partial\zeta, \quad h = H(x)+f'\int_{\zeta}^{\infty} \partial\theta/\partial y\, d\zeta \qquad (11a, b)$$

and made unique by the condition that it should vanish as $\zeta \to \infty$. The structure of the side layer is therefore determined by the equations

$$\partial^2\phi/\partial y^2 = \partial^4\phi/\partial\zeta^4, \quad \partial^2\theta/\partial y^2 = \partial^4\theta/\partial\zeta^4 \qquad (12a, b)$$

with the boundary conditions

$$\partial\phi/\partial\zeta = \partial\theta/\partial\zeta = \partial\phi/\partial x + f'\partial\theta/\partial y = \partial F/\partial y - \partial(f'G)/\partial x = 0 \quad \text{at} \quad \zeta = 0, \qquad (13a, b, c, d)$$

$$\phi \mp \theta = \partial^2\phi/\partial\zeta^2 \mp \partial\phi/\partial y \pm f'^2(\partial^2\theta/\partial\zeta^2 \mp \partial\theta/\partial y) = 0 \quad \text{at} \quad y = \pm f(x), \qquad (14)$$

$$\phi = \theta = 0 \quad \text{as} \quad \zeta \to \infty,$$

where F and G are the unknown values of $\partial^3\phi/\partial\zeta^3$ and $\partial^3\theta/\partial\zeta^3$ on $\zeta = 0$, these functions being even and odd in y respectively. The side-wall condition (8*d*) has been differentiated with respect to y in order to eliminate $H(x)$, which is ultimately determined by introducing the side-layer solutions for ϕ and θ into (8*d*) and (11*b*).

The analysis now follows the same path as in Part 2, so we shall omit details. With the introduction of cosine transforms equations (12) become a pair of ordinary differential equations in y with inhomogeneous terms containing F and G and with transformed boundary conditions (14) at $y = \pm f(x)$. This problem can be solved and inverted to get ϕ and θ in terms of F and G. In particular, at $\zeta = 0$, we have

$$\left.\begin{aligned} &\phi = \tfrac{1}{2}f^{-1}(R(+\hat{Y})+R(-\hat{Y})), \quad \theta = \tfrac{1}{2}f^{-1}(R(+\hat{Y})-R(-\hat{Y})), \\ &\text{where} \\ &R = \int_0^{\infty}\int_{-1}^{+1} r(x, Y)\,(\exp(-\Xi^2|\hat{Y}-Y|)-\bar{K}(\beta, \hat{Y}, Y, \Xi))\,\Xi^{-2}\,dY\,d\Xi, \\ &\bar{K} = \exp(-\Xi^2(2+\hat{Y}+Y))\,(1-\beta\exp(2\Xi^2\hat{Y}))/(1-\beta\exp(-2\Xi^2)), \\ &r = \pi^{-1}f^{\frac{1}{2}}(F+G), \quad \beta = (1-f'^2)/(1+f'^2), \quad \hat{Y} = yf^{-1}. \end{aligned}\right\} \qquad (15)$$

The boundary conditions (13*c*, *d*) did not enter the cosine-transform solution; together with the relationship (15) they now yield the pair of equations governing F and G.

Until this last step, the side-layer solution was identical to the one presented in §6 of Part 2. There the boundary conditions which were ignored by the cosine transform, namely

$$\phi = 1, \quad \theta = yf^{-1} \quad \text{at} \quad \zeta = 0,$$

gave a pair of integral equations for F and G which could be solved independently at each x section and which depended only on β. Since our governing conditions (13*c*, *d*) contain x derivatives, the local character of the previous solution has been lost and $f(x)$ must be given for all x (or suitable boundary conditions added at the ends of a finite interval) in order to determine the solution for any x.

We shall consider a duct with

$$f(x) = \begin{cases} a & \text{for} \quad x < 0, \\ a+bx & \text{for} \quad x > 0, \end{cases}$$

and in § 8 shall show how the solution for this prototype can be extended to a duct with any $f(x)$. In the present section we treat the portion with straight, diverging top and bottom walls ($x > 0$), in the next section we shall treat the constant-area portion ($x < 0$), and in § 5 we shall consider the free shear layer at $x = 0$ in order to join the upstream and downstream side-layer solutions.

The equation (13c) yields an integro-differential equation on r since f' and therefore β are constants. It is integrated with respect to $\hat{Y}$ from 0 to a new $\hat{Y}$ because $\partial\theta/\partial y$ gives an integral of r times $|\hat{Y}-Y|^{-\frac{1}{2}}\operatorname{sgn}(\hat{Y}-Y)$, which is too singular to be treated numerically. Since the integral equation

$$\int_{-1}^{+1} a(x)|y-x|^{\frac{3}{2}}\operatorname{sgn}(y-x)\,dx = 0$$

has a unique solution, $\quad a(y) = 0 \quad \text{for} \quad |y| \leqslant 1$

(Lundgren & Chiang 1967), we can multiply (13d) by $|\hat{Y}-Y|^{\frac{3}{2}}\operatorname{sgn}(\hat{Y}-Y)$ and integrate with respect to Y from -1 to $+1$ to get a second integro-differential equation for r. The equation derived from (13c) is odd in $\hat{Y}$ while the one from (13d) is even, so that they can be added without any loss of information to give

$$b^{-1}(a+bx)\int_{-1}^{+1} K_1(\hat{Y}, Y)\frac{\partial r}{\partial x}(x, Y)\,dY = \int_{-1}^{+1} K_2(\hat{Y}, Y)\,r(x, Y)\,dY$$
$$-(1-\beta)^{-1}(r(x,+1)+\beta r(x,-1))((1-\hat{Y})^{\frac{3}{2}}+(1+\hat{Y})^{\frac{3}{2}}), \quad (16)$$

where $\quad K_1 = |\hat{Y}-Y|^{\frac{3}{2}}\operatorname{sgn}(\hat{Y}-Y) - \tfrac{1}{2}(1-\beta)(\hat{K}_1(\hat{Y}, Y) - \hat{K}_1(-\hat{Y}, Y)),$

$$\hat{K}_1 = (2+\hat{Y}+Y)^{\frac{3}{2}} + 2\beta\pi^{-\frac{1}{2}}\int_0^\infty \exp(-\Xi^2(4+\hat{Y}+Y))(1-\beta\exp(-2\Xi^2))^{-1}$$
$$\times[(2+\hat{Y}+Y+2(1-\beta\exp(-2\Xi^2))^{-1})^2$$
$$+4\beta\exp(-2\Xi^2)(1-\beta\exp(-2\Xi^2))^{-2}]\,d\Xi,$$

$$K_2 = \tfrac{3}{2}(\beta(1-\beta)^{-1}+\hat{Y})|\hat{Y}-Y|^{\frac{1}{2}} + \tfrac{3}{2}(1-\beta)^{-1}|\hat{Y}+Y|^{\frac{1}{2}}$$
$$+\tfrac{3}{4}((1+\beta)-(1-\beta)\hat{Y})\hat{K}_2(\hat{Y}, Y) - \tfrac{3}{4}((1+\beta)+(1-\beta)\hat{Y})\hat{K}_2(-\hat{Y}, Y),$$

$$\hat{K}_2 = (2+\hat{Y}+Y)^{\frac{1}{2}} + 2\beta\pi^{-\frac{1}{2}}\int_0^\infty \exp(-\Xi^2(4+\hat{Y}+Y))(1-\beta\exp(-2\Xi^2))^{-1}$$
$$\times(2+\hat{Y}+Y+2(1-\beta\exp(-2\Xi^2))^{-1})\,d\Xi.$$

The integration by parts needed to eliminate the y derivative in (13d) gives rise to the last term in (16). This equation will be treated numerically in § 6.

4. Disturbed fully developed flow in a constant-area duct

The flow in an infinitely long constant-area duct is described by the two-dimensional fully developed solution of Shercliff (1953). The core variables are of $O(M^{-1})$ except for the $O(1)$ variables

$$U = 1, \quad \Phi = -z,$$

and the side layers are monotonic boundary layers matching the core and satisfying $u = 0$ at $\zeta = 0$. This flow is realized at $x \to -\infty$ in the constant-area portion ($x < 0$) of our prototypic duct, but is disturbed near $x = 0$ by side layers involving $O(M^{\frac{1}{2}})$ velocities, which are linked to the similar side layers in the diverging portion ($x > 0$).

Section 4.1 of Part 1 treats the core flow between two plane insulators at right angles to the applied magnetic field and the analysis given there is valid whatever the shape and nature of the side walls. The fundamental variables are again the $O(1)$ electric potential Φ and the $O(M^{-\frac{1}{2}})$ rescaled pressure H, which are now harmonic functions of x and z. The $O(1)$ core velocities are given by

$$U = -\partial\Phi/\partial z, \quad V = 0, \quad W = \partial\Phi/\partial x$$

and the $O(M^{-\frac{1}{2}})$ core currents are given by

$$J_x = \partial H/\partial z, \quad J_y = 0, \quad J_z = -\partial H/\partial x.$$

The conditions

$$\Phi = -z, \quad H = 0 \quad \text{as} \quad x \to -\infty$$

arise from matching the fully developed flow, and the other necessary boundary conditions arise from matching the side layers at $z = \pm 1$ and the free shear layer at $x = 0$.

The side layers are quite similar to those in the diverging portion, but we cannot obtain the governing integro-differential equation by simply setting $b = 0$ in (16). The kernels $\hat{K}_1$ and $\hat{K}_2$ involve integrals of $(1 - \beta \exp(-2\Xi^2))^{-1}$, which is singular at $\beta = 1$ and $\Xi = 0$. This singularity reflects a basic difference in the side-layer structure for $b = 0$. Since the flow is symmetric in z, we again consider only the side layer at $z = -1$. The governing equations (7a, b, c) and the side-wall conditions (8a, b, c, d) still hold, while the Hartmann conditions (9) become

$$v = \partial^2\phi/\partial\zeta^2 \mp \partial\phi/\partial y = 0 \quad \text{at} \quad y = \pm a \tag{17a,b}$$

and matching the core gives

$$v = 0, \quad \phi = \Phi(x, -1), \quad h = H(x, -1) \quad \text{as} \quad \zeta \to \infty. \tag{18a,b,c}$$

The boundary-value problem for ϕ is now decoupled from that for v and h except in the (ignored) wall conditions (8c, d). This problem cannot be solved using cosine transforms because the solution ϕ contains singularities at $\zeta = 0$, $y = \pm a$ which are not acceptable to the transforms. The basic operator in all of our side-layer problems is the product of the forward and backward diffusion operators $(\partial^2/\partial\zeta^2 \mp \partial/\partial y)$, so that any variable could be expressed as a superposition of heat-source solutions with $t = \pm y$. Normally these superposition solutions are useless because the boundary conditions at $y = \pm f(x)$ yield intractable integral equations involving unknown functions of x and ζ. However, for parallel top and bottom walls, the heat solutions automatically satisfy the decoupled conditions on ϕ at $y = \pm a$. In terms of F, again the unknown value of $\partial^3\phi/\partial\zeta^3$ on $\zeta = 0$, the correct solution is

$$\phi = \Phi(x, -1) - \int_{-a}^{a} F(x, y^*)\, \mathscr{L}(|y - y^*|, \zeta)\, dy^* + \tfrac{1}{2}(\mathscr{L}((a-y), \zeta) + \mathscr{L}((a+y), \zeta)) \int_{-a}^{a} F(x, y^*)\, dy^*,$$

where $$\mathscr{L}(y,\zeta) = \tfrac{1}{2}\zeta \operatorname{erf}(\tfrac{1}{2}\zeta y^{-\frac{1}{2}}) + \pi^{-\frac{1}{2}} y^{\frac{1}{2}} \exp(-\tfrac{1}{4}\zeta^2 y^{-1}).$$

The solution must satisfy $$\int_{-a}^{a} \partial\phi/\partial x(x,y,0)\,dy = 0$$

in order to be compatible with equation (7b) and boundary conditions (17a), (18b) and (8c). Together with the condition

$$\phi = \Phi(x,-1) = 1 \quad \text{as} \quad x \to -\infty,$$

this condition gives

$$\Phi(x,-1) = 1 - \tfrac{1}{3}a^{-1}\pi^{-\frac{1}{2}} \int_{-a}^{a} F(x,y^*)\,(2(a-y^*)^{\frac{3}{2}} - (2a)^{\frac{3}{2}})\,dy^*.$$

We again express v and h in terms of a potential function [cf. equations (11)]:

$$v = -\partial\theta/\partial\zeta, \quad h = H(x,-1) + \int_{\zeta}^{\infty} \partial\theta/\partial y\,d\zeta. \tag{19a,b}$$

Then θ satisfies (12b) and the boundary conditions

$$\theta = 0 \quad \text{at} \quad y = \pm a \quad \text{and} \quad \text{as} \quad \zeta \to \infty,$$

$$\partial\theta/\partial\zeta = \partial\phi/\partial x + \partial\theta/\partial y = \partial F/\partial y - \partial G/\partial x = 0 \quad \text{at} \quad \zeta = 0. \tag{20a,b,c}$$

Here G is the unknown value of $\partial^3\theta/\partial\zeta^3$ on $\zeta = 0$ and the wall condition (8d) has been differentiated with respect to y in order to eliminate $H(x,-1)$ which is ultimately determined by introducing the solutions for ϕ and θ into (8d) and (19b). Cosine transforms can be used to determine θ in terms of G and in particular at $\zeta = 0$ we find

$$\theta = (a^3/\pi)^{\frac{1}{2}} \int_{-1}^{+1} G(x,aY) \left(|\hat{Y} - Y|^{\frac{1}{2}} + \pi^{-\frac{1}{2}} \int_0^{\infty} \bar{L}(\hat{Y}, Y, \Xi)\,d\Xi \right) dY,$$

where $$\bar{L} = \exp(-\Xi^2)\sinh(\Xi^2\hat{Y})\sinh(\Xi^2 Y)/\Xi^2\sinh(\Xi^2), \quad \hat{Y} = y/a.$$

The wall conditions (20b,c) have not entered our analysis so far. As in §3 they now yield a single integro-differential equation

$$\int_{-1}^{+1} L_1(\hat{Y}, Y) \frac{\partial s}{\partial X}(X,Y)\,dY = \int_{-1}^{+1} L_2(\hat{Y}, Y)\,s(X,Y)\,dY - (s(X,+1) + s(X,-1))\,((1-\hat{Y})^{\frac{3}{2}} + (1+\hat{Y})^{\frac{3}{2}}), \tag{21}$$

where

$$L_1 = 2|\hat{Y} - Y|^{\frac{3}{2}} \operatorname{sgn}(\hat{Y} - Y) - \hat{Y}(1-Y)^{\frac{3}{2}} - \hat{Y}(1+Y)^{\frac{3}{2}} - (1+\hat{Y})^{\frac{3}{2}} + (1-\hat{Y})^{\frac{3}{2}} + 2^{\frac{3}{2}}\hat{Y},$$

$$L_2 = 3|\hat{Y} + Y|^{\frac{1}{2}} + \tfrac{3}{2}(2+\hat{Y}+Y)^{\frac{1}{2}} - \tfrac{3}{2}(2-\hat{Y}+Y)^{\frac{1}{2}} - \tfrac{3}{2}(2+\hat{Y}-Y)^{\frac{1}{2}} + \tfrac{3}{2}(2-\hat{Y}-Y)^{\frac{1}{2}} - 3\pi^{-\frac{1}{2}} \int_0^{\infty} \bar{L}(\hat{Y}, Y, \Xi) \exp(-2\Xi^2)\,d\Xi,$$

$$s = a^{\frac{5}{2}}\pi^{-1}(F+G), \quad X = x/a.$$

In §5 we shall derive an integral relationship between the solutions of (21) and its counterpart (16) in the diverging portion, and in §6 we shall solve the three coupled equations numerically.

5. Joining the flows at the free shear layer

A free shear layer of $O(M^{-\frac{1}{2}})$ thickness spans the duct at $x = 0$, separating the cores in the diverging and constant-area portions. Following the analysis presented in §4.3 of Part 1, which dealt with such shear layers, we find that

$$\partial^2\phi/\partial y^2 - \partial^4\phi/\partial\xi^4 = 0, \quad u = -\partial\phi/\partial z, \quad v = 0, \quad w = \partial\phi/\partial\xi,$$

$$j_x = -\partial^3\phi/\partial\xi^3, \quad j_y = \partial\phi/\partial y, \quad j_z = 0, \quad h = H(0^+) = H(0^-, z),$$

where the stretched co-ordinate is now $\xi = M^{\frac{1}{2}}x$ and ϕ, u, v, w, j_x, j_y, j_z and h denote the coefficient functions of the leading $O(1)$, $O(1)$, $O(M^{\frac{1}{2}})$, $O(M^{\frac{1}{2}})$, $O(M^{-\frac{1}{2}})$, $O(1)$, $O(1)$ and $O(M^{-\frac{1}{2}})$ terms in their own expansions respectively. Note that the assumptions made in Part 1 are satisfied because the $O(1)$ current is zero in both portions of our duct. The solution ϕ, which satisfies

$$\partial^2\phi/\partial\xi^2 \mp \partial\phi/\partial y = 0 \quad \text{at} \quad y = \pm a$$

and matches the two core solutions as $\xi \to \pm\infty$, is once again a superposition of heat-source solutions:

$$\phi = \tfrac{1}{4}\Phi(0^-, z)\,[\operatorname{erfc}(\tfrac{1}{2}\xi(a-y)^{-\frac{1}{2}}) + \operatorname{erfc}(\tfrac{1}{2}\xi(a+y)^{-\frac{1}{2}})].$$

Thus the shear layer absorbs whatever $O(1)$ mass flux remains in the constant-area core at $x = 0^-$ and carries it in equal parts to the intersection regions at $z = \pm 1$, where it is turned to flow into the side layers in the diverging portion.

Matching the shear-layer solution yields the boundary conditions

$$\partial H/\partial z = 0 \quad \partial\Phi/\partial x = 0 \quad \text{at} \quad x = 0$$

on the harmonic functions H and Φ in the constant-area core. The first condition follows immediately from the $O(M^{-\frac{1}{2}})$ shear-layer pressure h, while the second requires a look at the boundary-value problem for the $O(M^{-\frac{1}{2}})$ correction $\hat{\phi}$ to the $O(1)$ electric potential ϕ in the shear layer. Matching the two core solutions yields

$$\hat{\phi} = \hat{\phi}(0^-, z) \quad \text{as} \quad \xi \to \infty, \quad \hat{\phi} = \hat{\phi}(0^+, z) + \xi\,\partial\Phi/\partial x(0^+, z) \quad \text{as} \quad \xi \to -\infty,$$

and these conditions will not be compatible with the equations and Hartmann conditions for $\hat{\phi}$ (which are the same as the ones for ϕ) unless the constant-area core satisfies the secondary boundary condition above. These conditions state that the pressure and tangential velocity are continuous across the shear layer.

At $z = -1$ the shear layer intersects the side layer to form a region lying along the line $x = 0$, $z = -1$ from $y = -a$ to $y = a$ and having an $O(M^{-\frac{1}{2}}) \times O(M^{-\frac{1}{2}})$ cross-section. The details of the flow inside this region do not affect our solution elsewhere and will not be presented here. All we need to know is that $v = O(M^{\frac{1}{2}})$ and $j_y = O(1)$ in order to derive an equation relating our two side-layer solutions evaluated at $x = 0^{\pm}$. Since the area of any y section of this region is of $O(M^{-1})$, the vertical mass flux is of $O(M^{-\frac{1}{2}})$ and the vertical current flux is of $O(M^{-1})$. These being too small to redistribute either of the fluxes concerned, the integral of the

outward normal $O(M^{\frac{1}{2}})$ velocity or the outward normal $O(1)$ current density around a closed path in any y section must be zero. In particular

$$\int_0^\infty u(0^-, y, \zeta)\, d\zeta = \int_{-\infty}^\infty w(\xi, y, -1)\, d\xi + \int_0^\infty u(0^+, y, \zeta)\, d\zeta,$$

$$\int_0^\infty j_x(0^-, y, \zeta)\, d\zeta = \int_{-\infty}^\infty j_z(\xi, y, -1)\, d\xi + \int_0^\infty j_x(0^+, y, \zeta)\, d\zeta,$$

where the terms in each equation arise from the constant-area side layer, the shear layer and the variable-area side layer respectively. Introducing the expressions for the variables concerned in these regions yields the equations

$$\phi(0^-, y, 0) = \phi(0^+, t, 0), \quad h(0^-, y, 0) = h(0^+, y, 0)$$

joining the two side-layer solutions. We introduce the results of §3 and §4 into the first equation to obtain an integral relationship between $F(0^-, y)$, $F(0^+, y)$ and $G(0^+, y)$, which we integrate with respect to y from 0 to $\hat{y}$. We introduce the expressions (11b) and (19b) into the second equation and then differentiate it with respect to y in order to eliminate the constant, $H(0^-)$. The resulting equation, $G(0^-, y) = bG(0^+, y)$, is multiplied by $|\hat{y} - y|^{\frac{3}{2}} \operatorname{sgn}(\hat{y} - y)$ and integrated from $y = -a$ to $y = +a$ to obtain an integral relationship involving $G(0^+, y)$ and $G(0^-, y)$. Since these two relationships are odd and even in $\hat{y}$ respectively, they can be added without loss of information to obtain a single relationship

$$\int_{-1}^{+1} L_1(\hat{Y}, Y)\, s(0^-, Y)\, dY - \int_{-1}^{+1} K_3(\hat{Y}, Y)\, r(0^+, Y)\, dY = a\hat{Y}, \tag{22}$$

where $K_3 = (1+b)|\hat{Y} - Y|^{\frac{3}{2}} \operatorname{sgn}(\hat{Y} - Y) + (1-b)|\hat{Y} + Y|^{\frac{3}{2}} \operatorname{sgn}(\hat{Y} + Y)$
$$- (1-\beta)(\hat{K}_1(\hat{Y}, Y) - \hat{K}_1(-\hat{Y}, Y)).$$

In §6 we shall use this equation to join the solutions of the integro-differential equations (16) and (21) at $x = 0$.

6. Reduction to eigenvalue problems: numerics

If we assume solutions of the form

$$r = (a + bx)^{\gamma_i} r_i(Y), \quad s = \exp(\lambda_i X)\, s_i(Y)$$

for the important boundary-layer functions r and s defined in (15) and (21), the governing integro-differential equations (16) and (21) are reduced to eigenvalue problems independent of x. There is an infinite number of distinct eigenvalues for each equation, but we can exclude positive values of γ_i and negative values of λ_i because the corresponding functions are unbounded as $x \to \pm\infty$ respectively. The actual solution in each portion of the prototypic duct can be expanded in the remaining eigenfunctions, the coefficients in the two expansions being determined by joining them through (22). Since exact solutions have not been found we shall use a numerical scheme which is a close approximation.

We approximate the semi-infinite Ξ integrals in $\hat{K}_1$ and $\hat{K}_2$ with a Gauss quadrature from 0 to 1 and a Gauss–Hermite one beyond 1. The same scheme is

used for the intervals from Ξ_0 to $(1+\Xi_0)$ and beyond $(1+\Xi_0)$ for the integral in L_2, while the integrand is expanded for small Ξ and the resulting series is integrated term by term from 0 to Ξ_0, truncating after the Ξ_0^{12} term. If an n-point quadrature is used to approximate the integrals with respect to Y in (16), (21) and (22) and the continuous variable $\hat{Y}$ is only considered at n discrete values, then each equation becomes a set of linear equations involving the unknown values of r_i and s_i at the discrete Y values, which are the n abscissa for the quadrature. These Y values are also used for the discrete values of $\hat{Y}$ in order to cover the diagonal $\hat{Y} = Y$. Then γ_i and λ_i are the eigenvalues and $\mathbf{r}_i$ and $\mathbf{s}_i$ (n-vectors composed of the values of r_i and s_i at the discrete Y values) the eigenvectors of two $n \times n$ matrices. The n eigenvalues for each matrix approximate the n smallest (in absolute value) eigenvalues for the corresponding integral equation.

A 28-point extended Simpson's rule is used to determine the eigenvalues, this quadrature having abscissae at $Y = \pm 1$. The matrix equations are

$$\gamma_i \mathbf{K}_1 . \mathbf{r}_i = \mathbf{K}_2 . \mathbf{r}_i, \quad \lambda_i \mathbf{L}_1 . \mathbf{s}_i = \mathbf{L}_2 . \mathbf{s}_i,$$

where the $((1-\hat{Y})^{\frac{3}{2}} + (1+\hat{Y})^{\frac{3}{2}})$ terms in (16) and (21) have been incorporated into the first and last columns of $\mathbf{K}_2$ and $\mathbf{L}_2$. A standard QR algorithm is used to find the eigenvalues of the modified equations

$$((\mathbf{K}_1 + \mathbf{K}_2)^{-1} . \mathbf{K}_1) . \mathbf{r}_i = (1+\gamma_i)^{-1} \mathbf{r}_i, \quad (\mathbf{L}_2^{-1} . \mathbf{L}_1) . \mathbf{s}_i = \lambda_i^{-1} \mathbf{s}_i,$$

where γ_i has been shifted by adding $\mathbf{K}_1 . \mathbf{r}_i$ to both sides of the equation before inversion because the first eigenvalue is $\gamma_1 = 0$. In each set of 28 eigenvalues, 14 are acceptable, but we use only the first 12, since the last two are unreliable.

A 24-point Gauss quadrature with abscissae Y_j is used to determine the 12 corresponding eigenvectors $\mathbf{r}_i$ or $\mathbf{s}_i$ in each portion of the duct from

$$\mathbf{r}_i = (1-\beta)^{-1} (\mathbf{K}_2 - \gamma_i \mathbf{K}_i)^{-1} . \mathbf{V}, \quad \mathbf{s}_i = (\mathbf{L}_2 - \lambda_i \mathbf{L}_1)^{-1} . \mathbf{V},$$

where

$$\mathbf{V}_j = (1-Y_j)^{\frac{3}{2}} + (1+Y_j)^{\frac{3}{2}}.$$

The assumed values $r_1(+1) + \beta r_i(-1) = s_i(+1) + s_i(-1) = 1$ normalize the eigenvectors.

Using a 24-point Gauss quadrature to reduce the joining equation (22) to a set of approximate equations at discrete $\hat{Y}$ values and introducing the expansions

$$r(x, Y) = 2a\pi^{-\frac{1}{2}} \sum_{i=1}^{12} c_i a^{-\gamma_i} (a+bx)^{\gamma_i} r_i(Y),$$

$$s(X, Y) = 2a\pi^{-\frac{1}{2}} \sum_{i=1}^{12} d_i \exp(\lambda_i X) s_i(Y),$$

we obtain 24 linear equations which can be solved for the 12 unknown coefficients c_i in the expansion for the diverging portion and the 12 unknown coefficients d_i in the expansion for the constant-area portion. This completes the solution since the flow variables at any point in either portion can be written as the sum of twelve integrals of the eigenfunctions for that portion. The eigenvalues λ_i and the eigenfunctions s_i for the constant-area portion are the same for all a and b, while the eigenvalues γ_i and eigenfunctions r_i for the diverging portion, as well as all the coefficients c_i and d_i, depend only on b.

β								
+0·98	+0·9	+0·6	+0·3	+0·0	−0·3	−0·6	−0·9	−0·98
				b				
0·1005	0·2294	0·5000	0·7338	1·0000	1·3623	2·0000	4·3589	9·9500
				γ_i				
0·0	0·0	0·0	0·0	0·0	0·00	0·00	0·00	0·00
−33.2	−14·4	−6·8	−4·9	−3·89	−3·24	−2·75	−2·30	−2·14
−70·3	−30·8	−14·7	−10·6	−8·40	−6·95	−5·83	−4·78	−4·39
−113·8	−50·1	−23·9	−17·2	−13·62	−11·20	−9·31	−7·50	−6·82
−165·9	−73·1	−34·8	−25·0	−19·76	−16·17	−13·33	−10·60	−9·53
−229·1	−101·0	−48·1	−34·4	−27·08	−22·05	−18·05	−14·13	−12·62
−307·1	−135·4	−64·2	−45·9	−35·91	−29·09	−23·64	−18·29	−16·22
−405·4	−178·6	−84·5	−60·0	−46·77	−37·65	−30·35	−23·19	−20·42
−533·7	−235·0	−110·7	−78·2	−60·51	−48·29	−38·52	−29·00	−25·36
−710·7	−312·6	−146·5	−102·8	−78·81	−62·16	−48·82	−36·00	−31·21
−976·0	−482·8	−199·7	−139·1	−105·45	−81·84	−62·75	−44·70	−38·25
−1433·6	−629·2	−291·4	−201·3	150·80	−114·77	−84·89	−56·36	−47·04
				c_i				
0·0600	0·1381	0·2458	0·2543	0·2061	0·1205	0·0179	−0·0531	−0·0247
0·0419	0·1160	0·3001	0·4202	0·4728	0·4379	0·2886	0·0313	0·0264
0·0515	0·1445	0·3968	0·5879	0·6940	0·6535	0·3636	−0·2153	−0·4650
0·0290	0·0801	0·1950	0·2194	0·1038	−0·2430	−0·9556	−1·8469	−2·8701
−0·0403	−0·1181	−0·4219	−0·8667	−1·5200	−2·4464	−3·6490	−4·2714	−6·1816
−0·1230	−0·3496	−1·0846	−1·9080	−2·8355	−3·7774	−4·3875	−3·3117	−4·4433
−0·1384	−0·3817	−1·0344	−1·5109	−1·6856	−1·2485	0·4038	3·5225	4·9060
−0·0286	−0·0599	0·0921	0·7135	2·0216	4·3295	7·8819	10·1894	12·6440
0·1355	0·3972	1·4091	2·8073	4·6887	7·0151	9·2269	7·5948	8·1109
0·1909	0·5331	1·5690	2·5737	3·4457	3·8372	2·9079	−0·8911	−2·1642
0·1072	0·2904	0·7326	0·9598	0·8611	0·2032	−1·3501	−3·1076	−3·7501
0·0216	0·0568	0·1151	0·0846	−0·0621	−0·3571	−0·7709	−0·6231	−0·4823

				d_i				
0·0091	0·0218	0·0530	0·0835	0·1193	0·1662	0·2383	0·428	1·020
−0·0002	0·0008	0·0073	0·0169	0·0307	0·0510	0·0852	0·181	0·497
−0·0025	−0·0022	0·0148	0·0463	0·0952	0·1716	0·3057	0·694	2·029
−0·0106	−0·0131	0·0377	0·1452	0·3199	0·6015	1·1090	2·614	8·046
−0·0259	−0·0341	0·0835	0·3468	0·7865	1·5096	2·8351	6·851	22·139
−0·0422	−0·0543	0·1600	0·6434	1·4611	2·8227	5·3508	13·180	44·668
−0·0460	−0·0527	0·2418	0·8902	1·9911	3·8380	7·3018	18·285	64·980
−0·0285	−0·0233	0·2373	0·7875	1·7190	3·2881	6·2570	15·923	59·333
−0·0035	0·0000	0·0563	0·1682	0·3569	0·6754	1·2833	3·324	12·979
0·0041	−0·0172	−0·2208	=0·6067	−1·2500	−2·3372	−4·4329	−11·728	−47·878
−0·0054	−0·0507	−0·3710	−0·9480	−1·9020	−3·5211	−6·6891	−18·144	−76·781
−0·0115	−0·0540	−0·3076	−0·7517	−1·4897	−2·7582	−5·2809	−14·511	−62·034

TABLE 1. Eigenvalues and expansion coefficients

The values of γ_i, c_i and d_i for several values of $\beta = (1-b^2)/(1+b^2)$ are given in table 1, while the values of λ_i (which are independent of β) are 1·36, 5·34, 9·68, 14·80, 20·97, 28·58, 38·16, 50·67, 67·89, 93·67, 138·05 and 237·93.

The boundary conditions on the harmonic core variables $\Phi(x,z)$ and $H(x,z)$ in the constant-area portion are given by

$$\Phi(x, \pm 1) = \mp 1 \mp \tfrac{2}{3} \sum_{i=1}^{12} d_i \exp(\lambda_i x a^{-1}) \int_{-1}^{+1} s_i(Y)\,((1-Y)^{\frac{3}{2}} + (1+Y)^{\frac{3}{2}} - 2^{\frac{3}{2}})\,dY,$$

$$H(x, \pm 1) = -(\pi/a)^{\frac{1}{2}} \sum_{i=1}^{12} d_i \lambda_i^{-1} \exp(\lambda_i x/a) \int_{-1}^{+1} s_i(Y)\,dY,$$

while the core variable $H(x)$ in the diverging portion is given by

$$H(x) = -(\pi/a)^{\frac{1}{2}} \sum_{i=1}^{12} d_i \lambda_i \int_{-1}^{+1} s_i(Y)\,dY + (\pi/a)^{\frac{1}{2}} b^{-1} \sum_{i=1}^{12} c_i \{[a/(a+bx)]^{\frac{3}{2}-\gamma_i} - 1\} \times \left(2(1-\beta)^{-1}(\tfrac{3}{2}-\gamma_i)^{-1} - \int_{-1}^{+1} r_i(Y)\,dY\right).$$

Once the first two expressions have been evaluated, we can easily determine the constant-area core functions Φ and H, using a relaxation scheme for example, but these results, along with the expansions for the side-layer variables in both portions and the eigenvectors r_i and s_i, are of no great interest. However, in the next section we shall consider the division of the mass flux at $x = 0^-$ and the asymptotic form of the solution as $x \to \infty$, which has been called the quasi-developed flow (Walker 1970).

7. Mass flux division at $x = 0^-$ and quasi-developed flow

The flow in the prototypic duct consists of two flows which are independent of x, namely the fully developed flow in the constant-area portion and the quasi-developed flow given by $r = 2a\pi^{-\frac{1}{2}} c_1 r_1(Y)$ in the diverging portion, together with transition effects in the neighbourhood of the join at $x = 0$. In the diverging portion the transition effects just modify the existing high velocity side layers of the quasi-developed flow and die out like x^{γ_2}, where $\gamma_2 < -2$ for all β. In the constant-area portion, the transition effects create high velocity side layers which do not exist in the fully developed flow, these layers dying out like $\exp(1{\cdot}36x/a)$. Note how rapidly the disturbance caused by the join dies out in both directions.

In the diverging portion the mass flux is confined to the thin side layers by strong outward Lorentz forces produced by the $O(1)$ electrical currents flowing in the $\pm x$ direction within the side layers at $z = \pm 1$. As x increases the side layers spread out, becoming less severe and requiring less current, so that current lines are closed across the core through the $O(M^{-\frac{1}{2}})\,J_z$ associated with $H(x)$. The current lines must also close somewhere in the negative x direction and this is the origin of the high velocity layers in the constant-area portion. The circuit cannot be completed in the free shear layer because j_z is of $O(M^{-\frac{1}{2}})$ there, and it cannot be directly completed through the constant-area core because

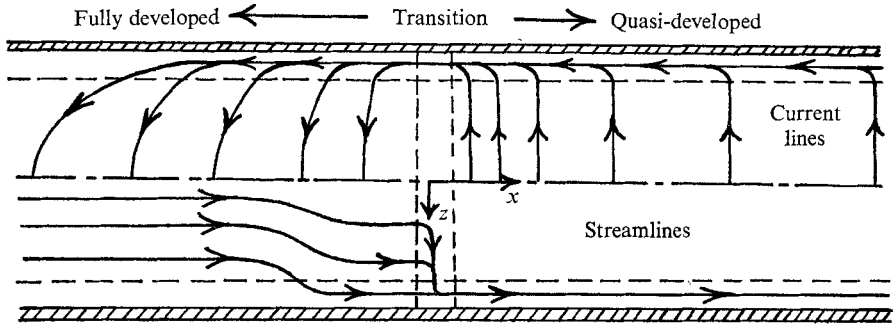

FIGURE 3. y section showing current lines and streamlines.

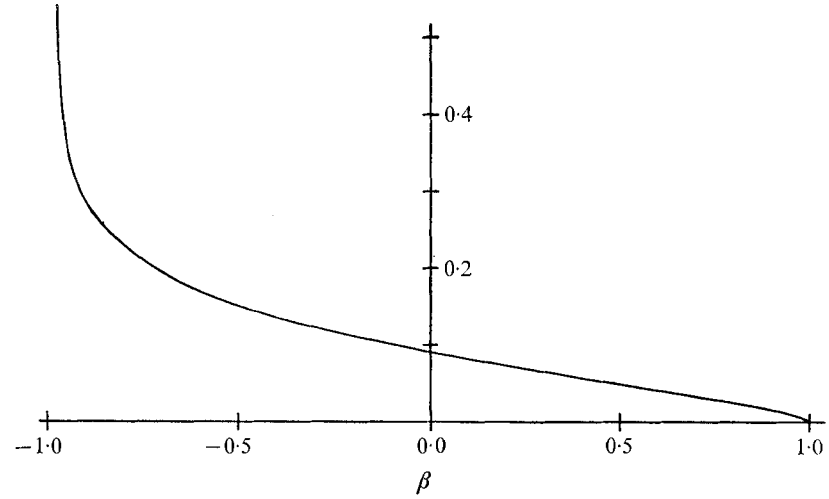

FIGURE 4. Fraction of the total mass flux carried by both side layers at $x = 0^-$.

the distribution of current flux in the side layers in the diverging portion varies with y while the distribution in the constant-area core is independent of y. Thus the currents travel along the side walls in the constant-area portion far enough for the side layers to redistribute the current flux in the y direction and to feed it into the core, where the circuit is closed by a plane potential current flow across the duct. In the process the Lorentz forces exerted by the currents in the side layers draw fluid into the layers, thereby absorbing part of the mass flux. Some possible streamlines and current lines for the plane $y = 0$ are sketched in figure 3. Some physical insight into the transition effects is gained from computing the fraction of the total mass flux carried by the two side layers as they enter $x = 0^-$, and this fraction is plotted as a function of β in figure 4. Note how the severity of the disturbance increases with b.

The side-layer variables in the quasi-developed solution can be written as powers of $(a+bx)$ times profile functions of $\beta = (1-b^2)/(1+b^2)$, $Y = y/(a+bx)$ and $Z = \zeta/(a+bx)^{\frac{1}{2}}$, namely

$$u = a(a+bx)^{-\frac{3}{2}}u^*, \quad v = ab(a+bx)^{-\frac{3}{2}}v^*, \quad w = ab(a+bx)^{-2}w^*,$$
$$j_x = ab(a+bx)^{-2}j_x^*, \quad j_y = a(a+bx)^{-2}j_y^*.$$

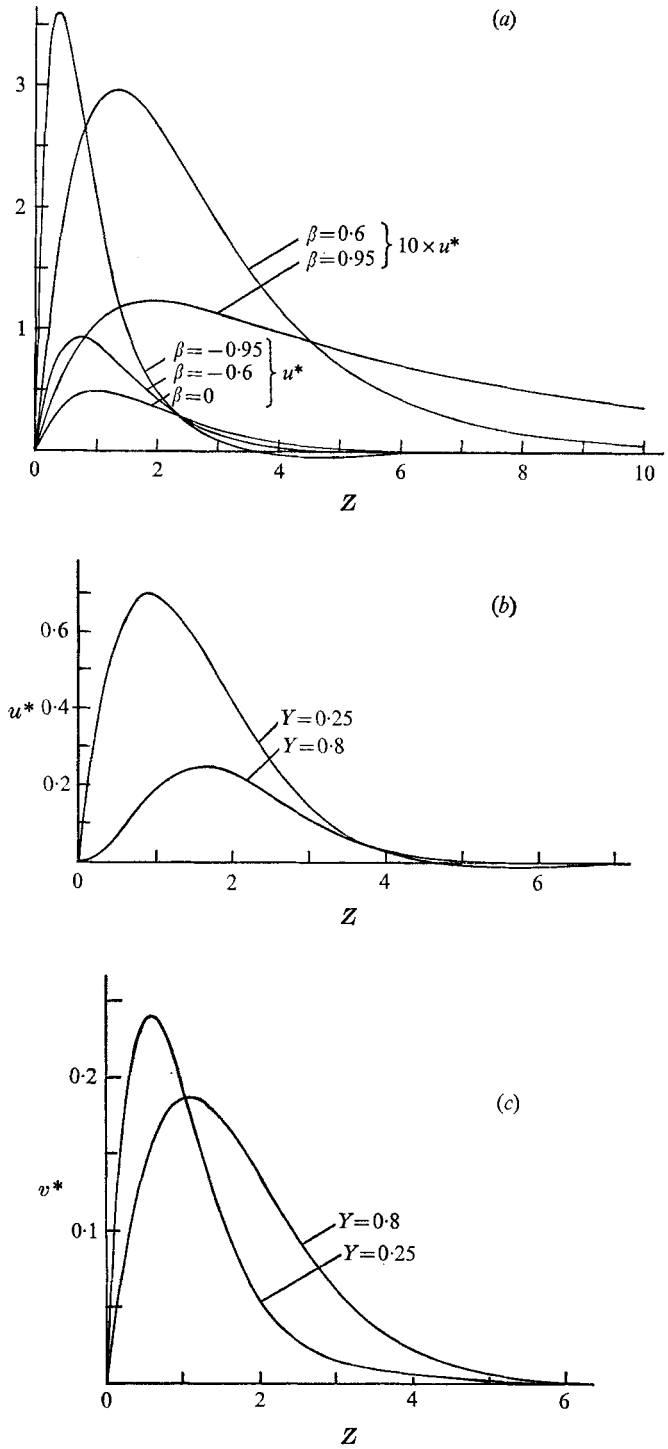

FIGURE 5 (*a–c*). For legend see facing page.

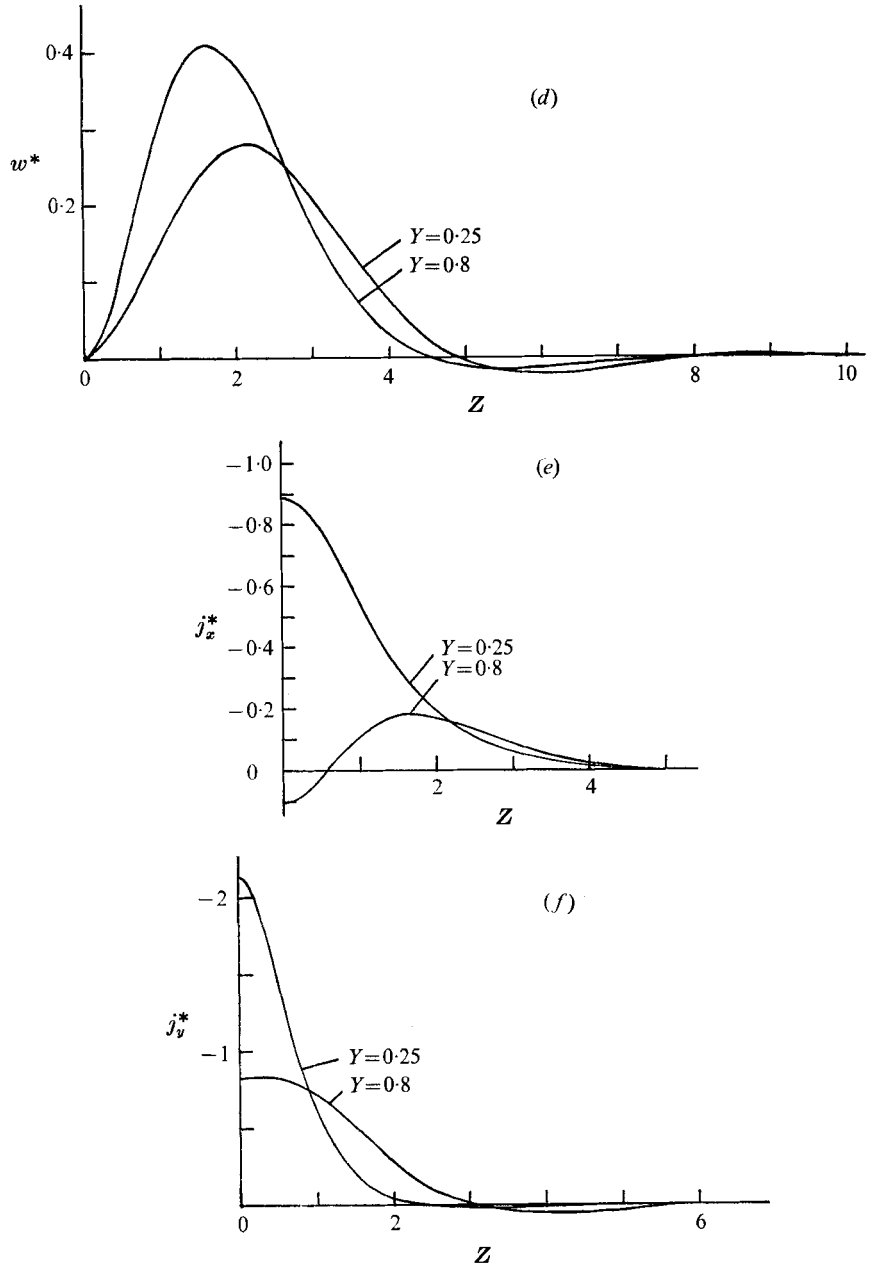

FIGURE 5. Typical side-layer profiles for quasi-developed flow. Profiles in (*a*) are for various values of β; all other profiles are for $\beta = -0{\cdot}6$.

Several typical profiles are presented in figure 5. Figure 5 (*a*) shows the variation with β of the velocity u on the line of symmetry $y = 0$. The other plots in figure 5 give the profile functions at the levels $Y = 0{\cdot}25$ and $0{\cdot}80$ for $b = 2$ ($\beta = -0{\cdot}6$).

8. Extensions

With the substitutions

$$x = -x, \quad u = -u, \quad j_x = -j_x, \quad z = -z, \quad w = -w, \quad j_z = -j_z,$$

the present solution becomes the solution for a semi-infinite converging duct with straight walls joined to a constant-area duct, that is, a duct with parallel side walls at $z = \pm 1$ for all x and with top and bottom walls at $y = \pm(a - bx)$ for $x < 0$ and at $y = \pm a$ for $x > 0$. The extension to ducts with converging or diverging side walls at $z = \pm g(x)$ is almost as easy. For ducts with perfectly conducting side walls, Part 2 showed that the flow for parallel side walls is radically different from that for diverging side walls. With parallel side walls the $O(1)$ transverse core current passes straight through the side layers without affecting their structure. With diverging side walls however these current lines must bend sharply inside the side layers in order to enter the conductors at right angles. These sharp bends create $O(M^{\frac{1}{2}})$ velocities in the side layers, which now carry a portion of the $O(1)$ mass flux. For the present duct with insulating side walls, the transverse core current is blocked by both parallel and diverging walls, and there is no fundamental difference between the two solutions. The half-width at $x = 0$ is used as the characteristic length so that $g(0) = 1$ and the mass flux condition (2) still holds. For $x > 0$ both pairs of walls are diverging, the $O(1)$ core solution vanishes and high velocity boundary layers which follow the side walls carry the entire mass flux. For the boundary layer at $z = -g(x)$ we introduce a set of orthogonal curvilinear co-ordinates $(\tilde{x}, y, \tilde{z})$ where $\tilde{z}$ is measured along the normal to the side wall. With the substitutions $x = \tilde{x}$ and $\zeta = M^{\frac{1}{2}}\tilde{z}$, our solution for the downstream side layers in a duct with parallel side walls becomes the corresponding solution for diverging side walls. An identical procedure gives the structure of the side layers for $x < 0$, since this structure is independent of the upstream core solution and is determined by matching the downstream side layers at $x = 0$. The upstream core variables Φ and H are once again harmonic functions of x and z which must satisfy the same boundary conditions at $x = 0$ and as $x \to -\infty$, and must match $\Phi(x, \pm g(x))$ and $H(x, \pm g(x))$, which are determined by the upstream side-layer solution.

The first important extension is to a variable-area duct with straight walls but finite length l, placed between two constant-area ducts ($y = \pm a$ for $x < 0$, $y = \pm(a + bx)$ for $0 < x < l$, $y = \pm(a + bl)$ for $x > l$). We allow realistic contractions as well as expansions by admitting negative values of $b > -a/l$. We again expand the solution for $x < 0$ in the eigenfunctions corresponding to the first m ($= 12$ in §6) positive eigenvalues of (21), and we expand the solution for $x > l$ in the eigenfunctions corresponding to the first m negative eigenvalues of the same equation, which in fact have the same absolute values as the positive eigenvalues. To expand the solution for $0 < x < l$ we use the eigenfunctions of (16) corresponding to the first $2m$ eigenvalues of either sign. There are a total of $4m$ unknown coefficients in the three expansions which are determined by applying the joining (22) at both $x = 0$ and $x = l$. The extension to a general variable-area duct with top and bottom walls at $y = \pm f(x)$ is now obvious. The variable-area

portion is divided into n segments, and the curved walls within each segment are approximated by straight walls with slopes b_i. The solution in each segment is expanded in all $2m$ eigenfunctions of (16) with $\beta = (1-b_i^2)/(1+b_i^2)$, and the $2m(n+1)$ unknown coefficients are determined by applying a joining equation like (22) at the entrance and exit of the variable-area portion and at each break in slope within this portion.

For $b = 0$ we have a constant-area duct for all x and there is fully developed flow everywhere. To complete the study of fully insulated variable-area rectangular ducts, we must see how such a radically different solution as the present one (with its blocked core flow for $x > 0$) evolves into the fully developed solution as $b \to 0$. This requires some care since several transitional stages are involved between $b = 0(1)$ and $b = 0$. These will be presented in Part 4, which is to appear in this journal.

Finally, as Hunt & Hancox (1971) have pointed out, very little is known about MHD flows in ducts (even of constant area) along which the applied magnetic field varies. The problem is of interest in design studies of cooling circuits for fusion reactors. Currents again tend to circulate in planes perpendicular to the magnetic field so that, when the walls are non-conducting, similar phenomena may be expected.

This research was supported partly by the U.S. Army Research Office-Durham and partly by the National Science Foundation under Grant GP-28483.

REFERENCES

BRANOVER, G. G. & SHCHERBININ, E. V. 1966 Magnetohydrodynamic jet flow in a bounded space. *Magnitnaya Gidrodinamika*, **2**, 55–63.

HUNT, J. C. R. & HANCOX, R. 1971 The use of liquid lithium as coolant in a toroidal fusion reactor. *U.K.A.E.A. Rep.* CLM-R115.

HUNT, J. C. R. & LUDFORD, G. S. S. 1968 Three-dimensional MHD duct flows with strong transverse magnetic fields. Part 1. Obstacles in a constant-area channel. *J. Fluid Mech.* **33**, 693–714.

HUNT, J. C. R. & SHERCLIFF, J. A. 1971 Magnetohydrodynamics at high Hartmann number. *Rev. Fluid Mech.* **3**, 37–62.

KULIKOVSKII, A. G. 1968 Slow steady state flows of conducting fluid at large Hartmann number. *Izv. Akad. Nauk S.S.R., Mekh. Zhid. i Gaza*, **2**, 3.

LUNDGREN, T. & CHIANG, D. 1967 Solution of a class of singular integral equations. *Quart. Appl. Math.* **24**, 303–313.

SHERCLIFF, J. A. 1953 Steady motion of conducting fluids in pipes under transverse magnetic fields. *Proc. Camb. Phil. Soc.* **49**, 136–144.

SLYUSAREV, N. M., SHILOVA, YE. I. & SHCHERBININ, E. W. 1970 Experimental study of converging and diverging MHD flow. *Magnitnaya Gidrodinamika*, **4**, 59–67.

WALKER, J. S. 1970 Three-dimensional magnetohydrodynamic flow in diverging rectangular ducts under strong transverse magnetic fields. Ph.D. thesis, Cornell University.

WALKER, J. S., LUDFORD, G. S. S. & HUNT, J. C. R. 1971 Three-dimensional MHD duct flows with strong transverse magnetic fields. Part 2. Variable-area rectangular ducts with conducting sides. *J. Fluid Mech.* **46**, 657–684.